Research Article | Vol. 28, No. 5 / 2 March 2020 / Optics Express 7274

Optics EXPRESS

Study of optical properties of graphene flakes and its derivatives in aqueous solutions

MILENA OJRZYNSKA,[1,*] ANNA WROBLEWSKA,[1] JAROSLAW JUDEK,[1] ARTUR MALOLEPSZY,[2] ANNA DUZYNSKA,[1] AND MARIUSZ ZDROJEK[1]

[1] *Faculty of Physics, Warsaw University of Technology, Koszykowa 75, 00-662 Warsaw, Poland*
[2] *Faculty of Chemical and Process Engineering, Warsaw University of Technology, 1, Waryńskiego Street, Warsaw 00-645, Poland*
[*] *milena.ojrzynska@pw.edu.pl*

Abstract: In this work, we study optical spectroscopy of graphene flakes and its derivatives such as graphene oxide and reduced graphene oxide in the same surfactant-free aqueous solution. We show that transmittance (T) and absorbance (A) spectra of different graphene suspension is nearly feature-less as a function of wavelength (λ) in the VIS-NIR range (350-1000 nm) except graphene oxide solution and the smallest graphene flakes, and they change linearly with concentration. The optical absorption coefficient (at 660 nm) of pure graphene solution seems to be flake-size dependent, changing from ~730 mL·mg^{-1}m^{-1} (for ~25 µm flake size) to ~4400 mL·mg^{-1}m^{-1} (for ~2 µm flake size), and it is several times higher than in the case of graphene oxide, which also varies with type and level of doping/defects (checked by FTIR and statistical Raman spectroscopy). Finally, we show wavelength-dependent evolution of optical absorption coefficient in the VIS-NIR range, which is roughly mimicking the A(λ) function but is strongly material-dependent. Our study could be useful for application of graphene solution in optofluidic devices, functional inks or printed flexible optoelectronics.

1. Introduction

Graphene-like materials in different forms (nanosheets, epitaxial films) can be produced with many different methods employed accordingly depending on final application [1]. One of the most widely used methods to obtain large quantities of 2D flakes is liquid phase exfoliation (LPE), resulting in breaking down multilayer graphite into single ones using ultrasound and/or shear forces in aqueous medium [2–5]. Interest in aqueous graphene dispersions is driven by the requirement for many different applications, such as optofluidic optical limiting devices [6,7,8], conductive inks [9], thermal fluids [10] or additives in composites [11]. Similarly, graphene derivatives – graphene oxide (GO) and reduced graphene oxide (rGO) – in aqueous solution are also attractive for many potential application, e.g. printed electrodes and flexible electronic devices [12], solar cells [13,14] or biosensors [15]. While many interesting works have been carried out on production of graphene flakes and its derivatives in liquid medium [2–5], for many applications it will be necessary to fully understand the physical properties of produced nanosheets in solutions, among others the optical properties, which seems to be not trivial [16]. Interestingly, optical characterization such as transmission or absorption coefficient can also serve as a feedback to optimize the dispersion and exfoliation processes of graphene flakes in liquid medium, since their size, defects and concentration, define the properties (not only optical) of the whole solution.

Optical absorption spectroscopy of graphene flakes suspension with surfactants produced by high-yield LPE was extensively employed by Coleman's group [4,5,17,18]. Using absorption coefficient (α) for given wavelength (here 660 nm) and the Beer-Lambert law [5] they extracted concentration of the nanosheets in the dispersion. For collecting the optical data a spectrometer with integral sphere has been used [5], which is an important point, failing which gives the α

#382523 https://doi.org/10.1364/OE.382523
Journal © 2020 Received 14 Nov 2019; revised 14 Jan 2020; accepted 3 Feb 2020; published 26 Feb 2020

Optics EXPRESS

significantly overestimated. In their work absorption coefficient at the wavelength of 660 nm for graphene in SDBS was calculated to be $<\alpha_{660}> = 1390$ mL mg^{-1} m^{-1}. For other surfactants, such as NMP, GBL, DMA and DMEU, an average absorption coefficient was $<\alpha_{660}> = 2460$ mL mg^{-1} m^{-1} [4]. Other works studying properties of aqueous-based graphene solutions (see Ref. [19] and references within) show extremely large variability of absorption coefficients, compared only for λ=660 nm but with many different solvents and experimental setups. The values start from $<\alpha_{660}> = 710$ mL mg^{-1} m^{-1} in aqueous sodium cholate and reach up to $<\alpha_{660}> = 6600$ mL mg^{-1} m^{-1} in water [19,20]. The reasons of such discrepancy are still not fully understood.

The study of absorption coefficient for reduced graphene oxide and graphene oxide in liquid solutions is literally closed only in few works and the data have been collected using equipment without integral sphere, and additionally the results vary a lot. Su et al. [21] show the value of α_{660} for rGO in NMP based solution is 3-5 orders of magnitude higher as compared to those for other graphene-based solution reported by others [4,7,21,22] and in this work. For graphene oxide samples the α_{660} shows more reasonable values (few thousand mL mg^{-1} m^{-1}), in the same order of magnitude reported in literature [20,23]. We note, that in the case of GO and rGO samples no results of absorption coefficient as a function of wavelength have been demonstrated so far.

Only the full information on optical properties in broad wavelength range can give comprehensive information about the graphene-based solution dedicated for above mentioned application. In this work, we provide an extensive comparative study on the optical properties of six surfactant-free aqueous solution based of commercially available graphene materials. We show the dependence of optical transmittance and absorption spectra on wavelength in the VIS-NIR range (350-1000 nm). We also demonstrate that optical absorption coefficient (in given optical range) is strongly dependent on the size of flakes in case of graphene and it is order of magnitude larger for different GO/rGO samples, while the different surfactant effect is being excluded by using only water/alcohol solution.

2. Experimental

For pure graphene suspensions three different flake size graphene powder has been used (Sigma Aldrich 25 µm particle size, surface area 120-150 m^2/g; Sigma Aldrich 5 µm particle size, surface area 50-80 m^2/g; Sigma Aldrich 2 µm particle size, surface area up to 500 m^2/g) and prepared by mixing graphene flakes with water and isopropanol (7:3) as a solvent. After ultrasound and centrifugation, part of solution was subjected to vacuum filtration [5] to determine the concentration (refers to highest concentration used) and next filter was weighed before and after filtration, what gives us average weight of material per milliliter of the filtered solution. The rest of the initial solution was subsequently diluted in order to get 5 different decreasing concentrations. For sake of clarity graphene solution from now on are named: $G_{2\mu m}$, $G_{5\mu m}$ and $G_{25\mu m}$ (to reflect different average size of the flakes). The size of the flakes was additionally confirmed by AFM study.

Graphene oxide water dispersion purchased from commercial manufacturer Graphenea (www.graphenea.com) in concertation 4 mg/mL, and was diluted in isopropanol and water (7:3) in such a way to get 5 different concentrations (samples named GO). An example of GO solutions is shown in Fig. 1(a). SEM image of GO shows the flat structure with some nanosheets rippled and entangled with each other which is typical for the GO samples (data not shown). The reduced GO material used in this work was acquired from two different sources - one with a known concentration from Sigma Aldrich stabilized with poly(sodium 4-styrenesulfonate) dispersed in water (marked as rGO*) and the other one with unknown concentration made using hydrazine reduction treatment of GO from Nanomaterials LS (marked as rGO). During solution preparation both samples were subjected only to gentle ultrasound treatment, however for rGO sample a concentration determination procedure was employed, in the same way as for graphene flakes.

Optics EXPRESS

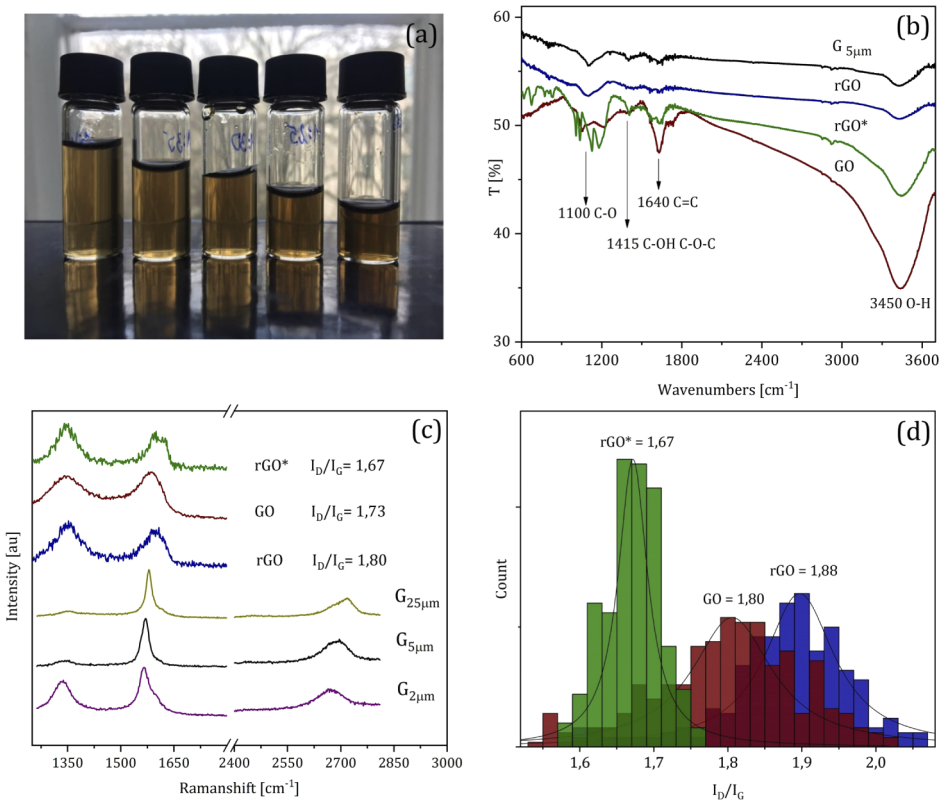

Fig. 1. (a) Picture of GO solutions with different concentration; (b) FTIR spectra (in transmittance mode) of GO, rGO*, rGO and also one of the graphene samples for comparison. (c) Single Raman spectra of graphene and its derivatives with I_D/I_G ratio indicated for each sample; (d) statistical I_D/I_G ratio for GO and two reduced graphene oxide samples

For Raman spectroscopy inVia Renishaw spectrometer with 532 nm laser source was used. The experiment was conducted at room temperature using low laser power (<1 mW) in order to avoid heating effects. The Raman mapping mode was used with scan area of ~50 × 50 µm, usually containing ~200 spectra. Each spectra in Fig. 1(c), containing two main bands (G an D), was fit using a Lorentzian line shape and extracted peak parameters for all spectra are presented as a histogram in Fig. 1(d).

FT-IR measurements were performed using Nicolet iS10 spectrometer (Thermo Fisher Scientific, USA) in transmittance mode and at room temperature condition. One milligram of each material: graphene, GO or rGO was mixed with 50 mg of KBr powder and pressed into the pellets. The spectrum was collected in the range 400-4000 cm^{-1} with a 4 cm^{-1} resolution.

Optical transmission measurements of all samples were recorded using a Bentham PVE300 spectral response analyser with integral sphere, using transmission configurations. Liquid samples of graphene-like flakes were transferred into quartz cuvettes with a 2 mm optical path and used for optical tests.

The results are presented as a quotient of sample with graphene transmission (T) and pure solvent sample (T_0) . Measured transmission was used to calculate absorbance defined as

$$A = -\log \frac{T}{T_0} \tag{1}$$

Optics EXPRESS

Beer's Law shown in Eq. (2) relates the attenuation of light to properties of a material. The law states the absorbance (A) is directly correlate to concentration (c) of dissolved material and path length (l) of the sample.

$$A = \alpha c l \tag{2}$$

The constant α is called absorption coefficient and it also is a measure of the probability of the electronic transition. Beer's Law is capable of describing the absorption behavior only if concentrations of solution are relatively low and directly proportional to the measured absorbance. High concentrations can cause different charge distribution in the solution and results in a shift in the absorption wavelength [30].

3. Results and discussion

As a starting point FTIR and Raman spectroscopy, were used in order to determine the quality, compare the oxidization level and check presence of functional groups in graphene-like flakes. Combination of these two methods is a powerful tool when performing materials characterization and is widely used to study properties of carbon nanostructures including graphene, GO and rGO [24,25,26].

The FTIR spectra of three samples – GO, rGO and rGO* are presented in Fig. 1(b). All spectra exhibit peak at 1100 cm^{-1} attributed to C-O bonding, then a peak at 1415 cm^{-1} that is related to C-OH or C-O-C bonds, the 1640 cm^{-1} peak related to carbonyl groups (C = O or C = C bonds). Additionally, a wide peak at 3450 cm^{-1} is present, indicating that sample contains water [27] and/or hydroxyl groups, and as expected is mostly pronounced for GO samples and barely visible for rGO and pure graphene. This is because, as a result of proper reduction of GO, some peaks should be completely removed and all intensities of peaks should be decreased, what is an indication of the removal of oxygen-containing functional groups. The FTIR spectra of rGO* in comparison to GO shows that peaks are in the same positions, their intensities are similar but we observed additional bands in the spectrum as shown in Fig. 2(a). Likely, this is because rGO* sample is only partly reduced and contains stabilizers, which gives additional bands in spectrum. Intensities of peaks in rGO are smaller than in GO and rGO* spectra so this sample contains less functional groups and it is more similar to $G_{5\mu m}$ sample. Furthermore, GO and rGO do not show features related to other impurities or additional surfactants.

The single Raman spectra of all graphene oxide and reduced GO samples together with an example of 'pure' graphene sample are shown in Fig. 1(c), exhibiting a defect-induced D-band at ~1350 cm^{-1} and G-band at ~1590 cm^{-1}, and for pure graphene additionally 2D band in seen (~2700 cm^{-1}). The occurrence of G band in Raman spectra corresponds to sp^2 hybridized carbon-based material. The D peak is related to defects and lattice disorder caused e.g. by oxygen-functional groups and its intensity is correlated with size of sp^2 in-plain domains [25]. First, we note that single spectra (and single I_D/I_G ratio) in case of large samples is insufficiently reliable and only statistical approach (histogram of I_D/I_G ratio) shown in Fig. 1(d) should be considered when we want to compare different graphene-like materials as can been seen in Figs. 1(c) and 1(d) rGO* spectra (green line and data) is representative for this material, whereas rGO and GO are much less reliable. Secondly, we note that, according to the literature the ratio I_D/I_G can be expected between 0.67-1.4 for more oxidized graphene material and 0.9-1.9 for more reduced GO [24,28], however these values are still under discussion. This may suggest that all our samples are more like rGO and that the reduction level in commercially available GO samples is significant, but on the other hand FTIR shows significant presence of functional groups within the material, which is shown as brown curve in Fig. 1(b). Nevertheless, both FTIR and Raman data show that level of doping/defects (reduction level) is much different for all studied samples.

Measured transmittance (T) and derived absorbance (A) spectra (in the range of 350-1000 nm) of all samples with different concentration are presented in the Fig. 2. It is clearly visible that values of $T(\lambda)$ of all samples with different concentrations decreases with increasing graphene

Optics EXPRESS

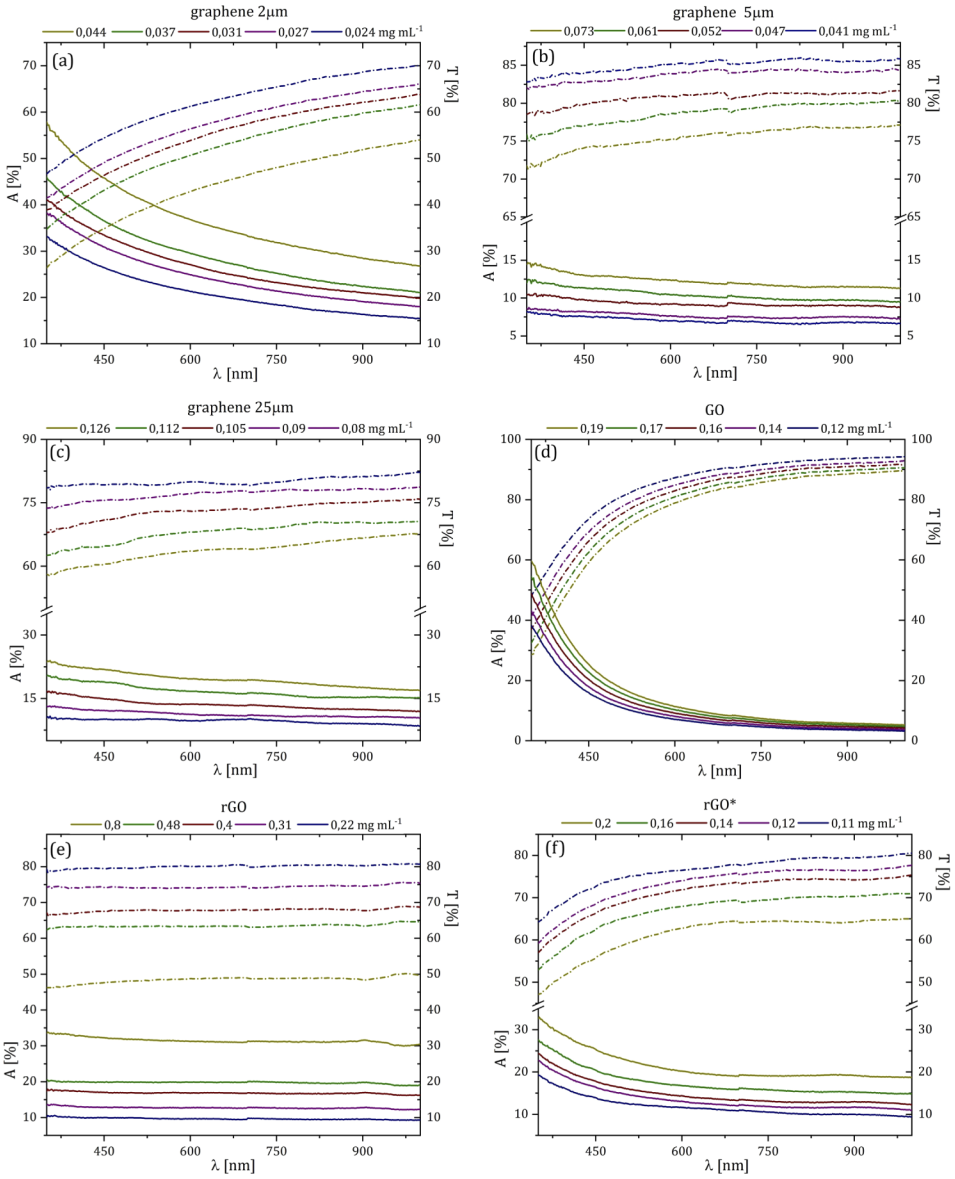

Fig. 2. Absorbance (solid lines) and transmittance (dash-dotted lines) spectra of solution as a function of wavelength in the range of 350-1000 nm containing different flakes with different concentration (mg/mL): (a) 2um size graphene, (b) 5um size graphene, (c) 25um size graphene flake, (d) graphene oxide (GO), (e) rGO and (f) rGO*.

material concentration, whereas A(λ) is increasing, as expected. However, the general trends of both parameters are material dependent. For example in Fig. 2(a) for 2 μm graphene absorption is decreasing with and λ by 20-30% (depending on concentration) within the full studied wavelength range. This effect could stem from: different sp^2/sp^3 ratio due to large number of flake edges or/and presence of C = O functional group, as shown in Fig. 1(c). Larger size graphene flake solutions are optically more stable in the sense that both absorption and transmission shown in Figs. 2(b) and 2(c), are nearly featureless and flat, showing only slight deviation for lower

Optics EXPRESS

wavelength. Similar (featureless) behaviour of T and A is observed for rGO samples in Fig. 2(d). The transmission of GO sample in Fig. 2(f) increases significantly (50-70%) up to around 750 nm and then remains at a nearly constant level of 90-97% depending on the concentration of the flakes and the absorbance shows maximum for lowest wavelength for all concentrations. Much smaller but still visible absorbance increase can be observed in spectra of rGO* in Fig. 2(e). It is likely that the increased absorption in UV region stems from effect of electron transfer from the non-binding orbital n to the π^* anti-bonding orbit due to the existence of carbonyl groups – carbon atom connected by a double bond to oxygen atom [29]. In both rGO* and GO samples the presence of large amount of functional groups has been confirmed by FTIR as shown in Fig. 1(b) and compared to other graphene-like samples.

Interestingly, assuming that absorbance is proportional to increase of graphene flakes (concentration) in a surfactant free solution, we can employ Lambert-Beer's law [30] in order to get a further insight in optical properties of different graphene materials, by deriving the absorption coefficient (α) in mL·mg^{-1}m^{-1} units. Usually, in the literature, the α is shown for fixed λ=660 nm [4,5,19,21], so here absorbance at 660 nm of incident light was divided by optical path length and presented as a function of determined concentration, as shown in Fig. 3(a). A slope of straight line fit through these points gives values of absorption coefficient for each sample. Those values are significantly different (more than an order of magnitude) depending on the samples. First tendency that can be noticed is the influence of the average flake size on the value of the α_{660}, which increases from ~730 mL·mg^{-1}m^{-1} for largest graphene flakes (25 µm) to more than 4400 mL·mg^{-1}m^{-1} for smallest fakes (2 µm). Despite large discrepancy between those values, they are still within the scope of those reported in literature, with the average value being ~2500 mL mg^{-1} m^{-1} [4]. We note again that our absorption coefficient is measured on surfactant-free solution, what additionally has impact on the optical properties.

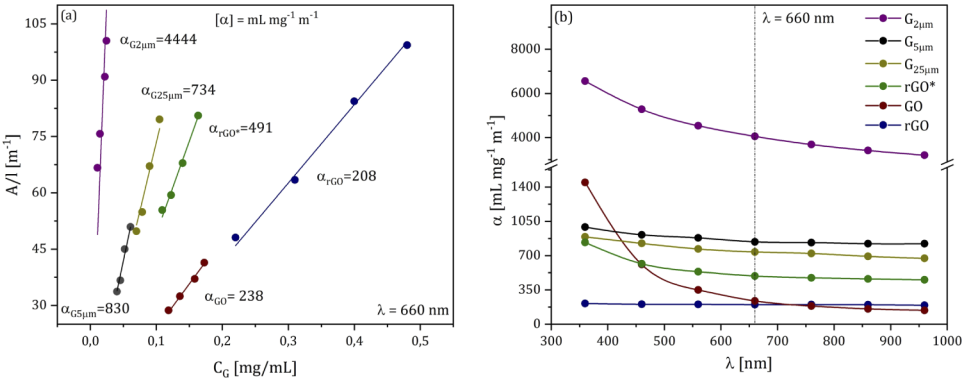

Fig. 3. (a) Absorbance divided by optical way at 660 nm as a function of concentration (after centrifugation) for all samples and determination of α_{660}. (b) Absorption coefficient α as a function of wavelength

The values of α_{660} for all three samples rGO*, rGO and GO sample are much smaller as compared to graphene. The lowest absorption coefficient (α_{660}=~200 mL·mg^{-1}m^{-1}) is seen for rGO sample (value very similar to GO sample), whereas the highest for rGO* sample - α_{660}=~500 mL·mg^{-1}m^{-1}.

The knowledge about optical absorption properties can be extended by looking at the evolution of absorption coefficient with the incident wavelength. The trend lines of $\alpha(\lambda)$ for all solutions are showed in Fig. 3(b) and are roughly mimicking absorbance spectra shown in Fig. 2. The α for GO solution (brown plot) shows strongly nonlinear behavior exhibiting the highest value for lowest wavelength and being low-flat (~200 mL mg^{-1} m^{-1}) above 650 nm. Also significant but

Optics EXPRESS

more smooth changes of $\alpha(\lambda)$, can be observed for smallest flake graphene (G_{2um}), that changes by 3000 mL·mg^{-1}m^{-1} within the studied wavelength range. The G_{25um} and rGO samples show rather featureless evolution of $\alpha(\lambda)$). In order to quantify these changes a ratio of absorption coefficient for two extreme wavelengths is calculated and shown in the Table 1. Factor $\alpha_{950}/\alpha_{350}$ shows how much the absorption coefficient of each graphene sample changes in a wide range of wavelength, so ratio close to 1 stands for most featureless evolution of $\alpha(\lambda)$.

Table 1. Ratio of absorption coefficient comparison in 950 nm and 350 nm. Factor $\alpha_{950}/\alpha_{350}$ shows how much the absorption coefficient changes as function of wavelength.

sample	$\alpha_{950}/\alpha_{350}$
rGO	**0,92**
G25µm	**0,83**
G5µm	**0,76**
rGO*	**0,54**
G2µm	**0,49**
GO	**0,098**

These results shows that taking appropriate graphene-like solution one can have the possibility of tuning the optical absorption for different wavelengths for quite wide range.

4. Conclusions

We have shown that wavelength-dependent optical absorption coefficient of graphene and its derivatives suspension are clearly material dependent. To demonstrate this we performed a comparative study of transmittance (T) and absorbance (A) in the 350-1000 nm range of different types of graphene-like materials. In particular, we showed that light absorption strongly depends on flakes size (especially for graphene) and/or reflects types and level of functionalization and defects present within the material.

To sum up, we conclude that variety of $\alpha(\lambda)$ for different graphene materials provides a rough overview for wide band tuning of optical properties in such applications as optical limiting material or optofluidic.

Funding

Narodowe Centrum Badań i Rozwoju (LIDER/33/0117/L-9/17/NCBR/2018); Fundacja na rzecz Nauki Polskiej (FNP Team-Tech grant (POIR.04.04.00-00-3C25/16-00)).

Disclosures

The authors declare no conflicts of interest.

References

1. E. P. Randviir, D. A. C. Brownson, and C. E. Banks, "A decade of graphene research: Production, applications and outlook," Mater. Today **17**(9), 426–432 (2014).
2. A. Ciesielski and P. Samorı, "Gaphene viasonication assisted liquid-phase exfolaition," Chem. Soc. Rev. **43**(1), 381–398 (2014).
3. V. Nicolosi, M. Chhowalla, M. Kanatzidis, M. S. Strano, and J. N. Coleman, "Liquid Exfoliation of Layered Materials," Science **340**(6139), 1226419 (2013).
4. Y. Hernandez, V. Nicolosi, M. Lotya, F. M. Blighe, Z. Sun, S. De, I. T. McGovern, B. Holland, M. Byrne, Y. K. Gun'Ko, J. J. Boland, P. Niraj, G. Duesberg, S. Krishnamurthy, R. Goodhue, J. Hutchison, V. Scardaci, A. C. Ferrari, and J. N. Coleman, "High-yield production of graphene by liquid-phase exfoliation of graphite," Nat. Nanotechnol. **3**(9), 563–568 (2008).

Optics EXPRESS

5. M. Lotya, Y. Hernandez, P. J. King, R. J. Smith, V. Nicolosi, L. S. Karlsson, F. M. Blighe, S. De, Z. Wang, I. T. McGovern, G. S. Duesberg, and J. N. Coleman, "Liquid phase production of graphene by exfoliation of graphite in surfactant/water solutions," J. Am. Chem. Soc. **131**(10), 3611–3620 (2009).
6. C. Fang, B. Dai, R. Hong, C. Tao, Q. Wang, X. Wang, D. Zhang, and S. Zhuang, "Tunable optical limiting optofluidic device filled with graphene oxide dispersion in ethanol," Sci. Rep. **5**(1), 15362 (2015).
7. G. K. Lim, Z. Chen, J. Clark, R. G. S. Goh, W. Ng, H. Tan, R. H. Friend, P. K. H. Ho, and L. Chua, "Giant broadband nonlinear optical absorption response in dispersed graphene single sheets," Nat. Photonics **5**(9), 554–560 (2011).
8. L. Yan, Y. Xiong, J. Si, X. Sun, W. Yi, and X. Hou, "Optical limiting properties and mechanisms of single-layer graphene dispersions in heavy-atom solvents," Opt. Express **22**(26), 31836 (2014).
9. M. S. Dandan Satia, M. Jaafar, and S. Fontana, "Recent Development of Graphene-Based Ink and Other Conductive Material-Based Inks for Flexible Electronics," J. Electron. Mater. **48**(6), 3428–3450 (2019).
10. M. Rodríguez-Laguna, A. Castro-Alvarez, M. Sledzinska, J. Maire, F. Costanzo, B. Ensing, M. Pruneda, P. Ordejón, C. Sotomayor Torres, P. Gómez-Romero, and E. Chávez-Ángel, "Mechanisms behind the enhancement of thermal properties of graphene nanofluids," Nanoscale **10**(32), 15402–15409 (2018).
11. K. Żerańska, A. Lapinska, A. Wróblewska, J. Judek, A. Duzynska, M. Pawlowski, A. Witowski, and M. Zdrojek, "Study of the absorption coefficient of graphene-polymer composites," Sci. Rep. **8**(1), 9132 (2018).
12. A. Ji, Y. Chen, X. Wang, and C. Xu, "Inkjet printed flexible electronics on paper substrate with reduced graphene oxide/carbon black ink," J. Mater. Sci.: Mater. Electron. **29**(15), 13032–13042 (2018).
13. S. Lee, J. Yeo, J. Yun, and D. T. Kim, "Water dispersion of reduced graphene oxide stabilized via fullerenol semiconductor for organic solar cells," Opt. Mater. Express **7**(7), 2487–2495 (2017).
14. Q. Yang, H. Li, Z. Guan, B. Yu, J. Li, and S. Tsang, "Graphene Oxide as Efficient Hole Transporting Material for High-Performance Perovskite Solar Cells with Enhanced Stability," J. Mater. Chem. A **5**(20), 9852–9858 (2017).
15. J. Peña-Bahamonde, H. Nguyen, S. Fanourakis, and D. Rodrigues, "Recent advances in graphene-based biosensor technology with applications in life sciences," J. Nanobiotechnol. **16**(1), 75 (2018).
16. K. R. Paton and J. N. Coleman, "Relating the optical absorption coeffcient of nanosheet dispersions to the intrinsic monolayer absorption," Carbon **107**, 733–738 (2016).
17. K. Paton, E. Varrla, C. Backes, R. Smith, U. Khan, A. Gallagher, C. Boland, M. Lotya, O. Istrate, P. King, T. Higgins, S. Barwich, P. Puczkarski, I. Ahmad, M. Möbius, H. Pettersson, E. Long, J. Coelho, and J. Coleman, "Scalable production of large quantities, defect-free few-layer graphene by shear exfoliation in liquids," Nat. Mater. **13**(6), 624–630 (2014).
18. J. Coleman, "Liquid Exfoliation of Defect-Free Graphene," Acc. Chem. Res. **46**(1), 14–22 (2013).
19. D. Ager, V. Arjunan Vasantha, R. Crombez, and J. Texter, "Aqueous Graphene Dispersions–Optical Properties and Stimuli-Responsive Phase Transfer," ACS Nano **8**(11), 11191–11205 (2014).
20. M. Yi, Z. Shen, X. Zhang, and S. Ma, "Achieving concentrated graphene dispersions in water/acetone mixtures by the strategy of tailoring Hansen solubility parameters," J. Phys. D: Appl. Phys. **46**(2), 025301 (2013).
21. R. Su, S. Fen Lin, D. Qing Chen, and G. Hua Chen, "Study on the Absorption Coefficient of Reduced Graphene Oxide Dispersion," J. Phys. Chem. C **118**(23), 12520–12525 (2014).
22. J. Guerrero-Contreras and F. Caballero-Briones, "Graphene oxide powders with different oxidation degree, prepared by synthesis variations of the Hummers method," Mater. Chem. Phys. **153**, 209–220 (2015).
23. D. Konios, M. Stylianakis, E. Stratakis, and E. Kymakis, "Dispersion behavior of graphene oxide and reduced graphene oxide," J. Colloid Interface Sci. **430**, 108–112 (2014).
24. A. Wróblewska, A. Duzynska, J. Judek, L. Stobinski, K. Leszek, A. Żerańska, M. Gertych, and Zdrojek, "Statistical analysis of the reduction process of graphene oxide probed by Raman spectroscopy mapping," J. Phys.: Condens. Matter **29**(47), 475201 (2017).
25. B. Tang, H. Guoxin, and H. Gao, "Raman Spectroscopic Characterization of Graphene," Appl. Spectrosc. Rev. **45**(5), 369–407 (2010).
26. V. Schiopu-Tucureanu, M. Alina, and A. Avram, "FTIR Spectroscopy for Carbon Family Study," Crit. Rev. Anal. Chem. **46**(6), 502–520 (2016).
27. Z. Çiplak, N. Yildiz, and A. Çalimli, "Investigation of Graphene/Ag Nanocomposites Synthesis Parameters for Two Different Synthesis Methods," Fullerenes, Nanotubes, Carbon Nanostruct. **23**(4), 361–370 (2015).
28. R. Rozada, J. Paredes, S. Villar-Rodil, A. Martínez-Alonso, and J. Tascón, "Towards full repair of defects in reduced graphene oxide films by two-step graphitization," Nano Res. **6**(3), 216–233 (2013).
29. S. Uran, A. Alhani, and C. Silva, "Study of ultraviolet-visible light absorbance of exfoliated graphite forms," AIP Adv. **7**(3), 035323 (2017).
30. H. K. Hughes, "Beer's Law and the Optimum Transmittance in Absorption Measurements," Appl. Opt. **2**(9), 937–945 (1963).